Chapter 27

Molecular Replica Symmetry Breaking

Felix Ritort*

Small Biosystems Lab
Department de Física de la Matèria Condensada
Facultat de Física, Universitat de Barcelona
Carrer de Martí i Franqués 1, 08028 Barcelona (Spain)
ritort@ub.edu,fritort@gmail.com†

A brief overview of mechanical unzipping experiments of single nucleic acids and proteins shows the power of single-molecule techniques to unravel molecular energy landscapes with kcal/mol accuracy. I argue that pulling experiments offer an ideal playground to explore rugged free-energy landscapes and replica symmetry breaking at the single-molecule level.

27.1. Biomolecules and spin glasses

Nucleic acids (NA) are found in double-stranded and single-stranded forms [1]. The DNA double helix comprises two covalently linked sugar-phosphate strands of nucleotides (see previous chapter by Cocco and colleagues) stabilized by base pairing and stacking interactions. RNA is mostly found in single-stranded form and participates in many regulatory processes in the cell. Chemically, RNA differs from DNA in that the nucleotide U-uracyl replaces T-thymine, and the sugar (ribose) in the phosphate chain contains a polarizable OH group that coordinates metal ions such as magnesium and calcium [2–4]. In contrast, proteins are chains of covalently linked amino acids that fold into specific three-dimensional shapes [5] with multiple structural, signaling, and enzymatic functions. Proteins catalyze a myriad of reactions essential for life.

NA and proteins are intrinsically disordered and heterogeneous, their extraordinary organizing power is due to the strong sensitivity of the monomer interactions to changes in sequence and environment. This sensitivity originates from the acute energy balance of molecular interactions in water. Multiple forces such as hydrogen bonding, Van der Waals, and the hydrophobic effect concur to fold biomolecules into the specific native structure, a free energy minimum in the space of conformations [6]. In thermodynamics, Gibbs free energy $G = H - TS$ results from the balance between enthalpy H (the equivalent of the potential energy in mechanics) and entropy S, a statistical measure of the disorder, with T the temperature. Minimizing G requires H minimum and S

*E-Mail:ritort@ub.edu
†Affiliation footnote.

maximum, which for molecular driving forces often leads to conflicting results. An example of the competition between H and S is the hydrophobic effect of non-polar molecules that repel water. In truth, it is the opposite effect; non-polar molecules tend to form stable hydrogen bonds with water (~ 7 kcal/mol per bond), yet this comes at the price of a large entropic cost of hydrogen-bonding alignment, so the overall free energy change is positive. Enthalpy-entropy compensation in molecular folding results in very low folding ΔG (positive) values compared to ΔH and $T\Delta S$, $\Delta G \ll \Delta H, T\Delta S$ with ΔH comparable to $T\Delta S$. For example, at room temperature $T = 25^{\text{o}}$C, the 110 amino acids ribonuclease protein barnase has a folding free energy value of $\Delta G = 10$ kcal/mol (kilocalories per mole) with $\Delta H \sim 115$kcal/mol, $T\Delta S = 105$ kcal/mol. Hydrogen bonds and Van der Waals forces are critical for folding. While hydrogen bonding mostly drives the formation of the transition state that precedes native folding, Van der Waals forces are responsible for closely packing nucleotides in NA and side chains in proteins. The large $1/r^6$ energy dependence of the latter contributes to the large energy collapse between the transition and the native state.

Structural rearrangements in NA and proteins lead to conflicting energy interactions and rugged free energy landscapes, a typical feature of spin glasses containing disorder and frustration. Two are the main differences though. While biomolecules are nanometer-sized, spin and structural glass samples are meso- and macroscopic. Moreover, evolutionary forces have built biomolecules into polymer chains that have a specific purpose or function, a feature absent in ordinary matter such as spin glasses (diluted random alloys) and structural glasses. Many structural glasses are homogeneous liquids that crystallize if cooled slowly enough. Otherwise, they enter the supercooled liquid region and a glassy phase [7]. Although covalent bonds determine the high viscous phase of glass-forming liquids such as pure silica (SiO_2), which crystallizes at 1475K, weak interactions also form glassy phases in organic substances and water [8].

Spin glasses, structural glasses, and disordered matter are characterized by rough free energy landscapes with many states, mathematically described by the replica symmetry breaking transition (RSB) in spin glass theory [9]. Can the remarkable thermodynamic and kinetic phenomena of replica symmetry breaking be observed at the molecular level in NAs and proteins? A primary tool to answer this question is single-molecule force spectroscopy, where an individual molecule can be mechanically pulled from its ends to monitor the folding reaction in real-time [10, 11]. Pulling experiments permit us to derive free energy differences by mechanical work measurements, mostly with laser optical tweezers and magnetic tweezers, atomic force cantilevers, acoustic sound waves, and others [12, 13].

27.2. Molecular free energy landscapes

In pulling experiments, the end-to-end distance x is a reaction coordinate that quantifies the progress of the hybridization reaction in a DNA duplex and the folding of an RNA or protein. In single-trap optical tweezers [14, 15], the molecule under study is inserted between flanking handles. The molecular construct is tethered between a surface and an optically trapped bead using specific linkages (Fig.27.1A). The trap-position distance λ

comprises the extension of the handles and the molecule under study x and the micron-sized bead displacement, $\lambda = x_b + x$. In this experimental setup, λ is the control parameter and does not fluctuate, whereas x and the force applied to the system, $f = k_b x_b$, fluctuate due to Brownian noise. Typically, the bead stiffness $k_b \sim 0.01 - 1\text{pN/nm}$ permits force measurements in the range $0.1 - 100\text{pN}$. By repeatedly moving the optical trap back and forth, we measure the force-distance curve (FDC), where the force f is plotted versus the distance λ. In unzipping experiments a DNA hairpin is tethered between the two extremities and the two strands pulled apart by mechanical forces [16, 17]. Figure 27.1B shows the FDC of unzipping a 6.8kbp DNA molecule at standard conditions ($T = 298\text{K}$, 1M NaCl). In the upper panel, we show the average FDC (black line) and the raw data (grey band) showing Brownian force fluctuations. In the bottom panel, the unzipping (grey) and rezipping (black) curves superimpose, showing that the unzipping-rezipping reaction is quasi-reversible [18].

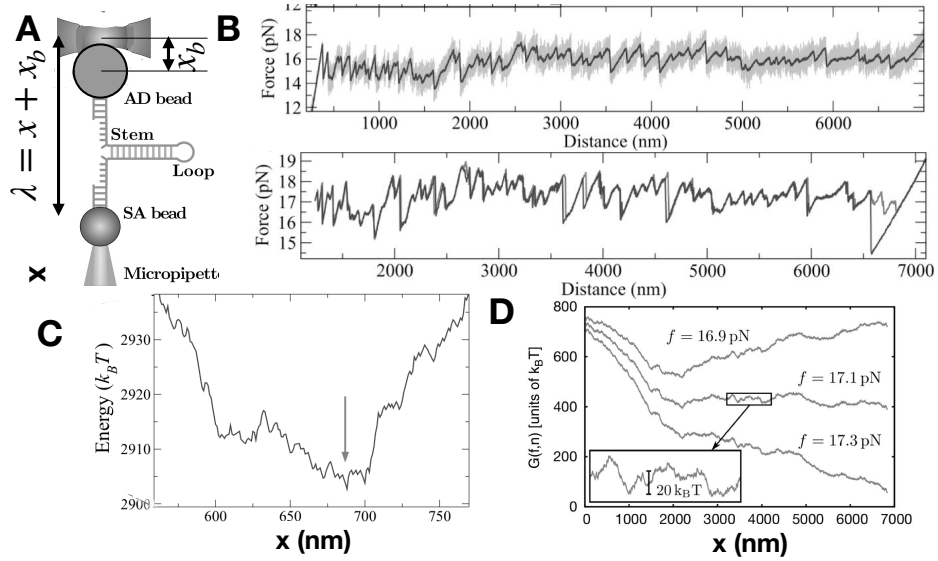

Fig. 27.1. Unzipping free energy landscapes. A) Experimental setup. B) Unzipping FDC of a 6.8kbp DNA hairpin. (Top) Filtered data at 1Hz (continuous black line) and raw data at 1kHz (grey band). (Bottom) Unzipping (grey) and rezipping (black) FDCs are near reversible, except for the effect of the refolding loop at the end. Data from Ref. [18] C,D) Free-energy landscapes in the trap-position ensemble $G_\lambda(x)$ for a given trap position λ and in the force ensemble $G_f(x)$.

For fixed λ, experimental measurements of the fluctuating extension x, permit us to extract the molecular free energy landscape, $G_\lambda(x)$, using the Boltzmann formula,

$$P_\lambda(x) = \frac{\exp(-\beta G_\lambda(x))}{Z_\lambda} \; ; \; G_\lambda(x) = -k_B T \log P_\lambda(x) - k_B T \log Z_\lambda \tag{27.1}$$

with Z_λ the equilibrium partition function. The constant $G_\lambda = -k_B T \log Z_\lambda$ is the equilibrium free energy of the molecule at λ, an overall shift to the free energy landscape. A typical unzipping free energy landscape $G_\lambda(x)$ for a given trap position λ is shown in Fig.27.1C. The profile has been calculated using the nearest neighbor (NN) model for DNA [19]. In the NN model, the free energy of the duplex is the sum of the stacking

and hydrogen bond interactions between all adjacent base pairs. The free energy is rough with many local minima, a feature of disordered and frustrated systems. From $G_\lambda(x)$ one can also calculate the free energy landscape in the force-ensemble where force is fixed, $G_f(x)$. This ensemble is implemented in magnetic tweezers where a pair of magnets produce a constant magnetic field gradient force. $G_f(x)$ for the 6.8kbp DNA is shown in Fig.27.1D for three force values, 16.9,17.1,17.3pN. Again, $G_f(x)$ is rough with many minima (inset) and energy barriers of roughly $20k_BT$.

The unzipping free energy landscape is an experimental realization of the 1D Sinai's model commonly used to illustrate spin-glass free energy landscapes. Unzipping measurements permit us to measure free energy differences by applying the thermodynamic identity, $\Delta G_\lambda = W$ with W the mechanical work exerted by the optical tweezers instrument on the molecule. By comparing the measured FDC with the theoretical prediction based on the NN model, the ten nearest-neighbor energy parameters have been derived over several decades of salt concentration in sodium and magnesium with 0.1kcal/mol accuracy [20, 21].

27.3. Barrier energy landscapes

Disorder and frustration also affect the folding kinetics of biomolecules [22]. RNAs form secondary structures made of single-stranded unpaired regions and stem loops stabilized by hydrogen bonds and stacking [23]. The promiscuity of base pairing in RNA is facilitated by non-Watson-Crick or wobble base pairs (such as GU) that enlarge the diversity of tertiary structures. The ribose C3'-endo conformation also makes RNA adopt the more compact A-form with stronger base stacking than for DNA. Upon folding, RNA can be kinetically trapped into structures other than the native (misfolding), a typical feature of glassy matter. In Figure 27.2A, we show unzipping curves at room temperature (T=298K) and 10mM $MgCl_2$ for a 2kbp RNA hairpin [24]. Compared to DNA (Fig.27.1B, bottom), hysteresis between the unzipping (grey) and rezipping (black) FDCs is apparent. Such irreversibility has been interpreted as due to competing off-pathway structures formed along the unpaired strands during the unzipping-rezipping reaction, Fig.27.2B [24, 25]. Segments of various lengths $L_1, L_2, .., L_k$ can be transiently stabilized at forces as high as 17pN. BEL minima are correlated with high hysteresis regions (e.g., Fig.27.2B, zoom).

The notion of the BEL finds its most natural example in Kramers theory of 1D systems. For a NA hairpin of N bases pulled at a force f, the kinetic rate of unfolding k_U is given by [27, 28],

$$k_U(f) = k_0 \exp\big(-\frac{B_U(f)}{k_BT}\big)\ ;\ \frac{B_U(f)}{k_BT} = \log\big(\sum_{m=0}^{N}\sum_{m'=0}^{m}\exp(\frac{G_m(f)-G_{m'}(f)}{k_BT})\big) \quad (27.2)$$

with k_0 an attempt rate, $B_U(f)$ the kinetic barrier, and $G_m(f)$ $(m = 0, 1, .., N)$ the free energy landscape at force f. For landscapes with a maximum at a force-dependent position $m = m^*(f)$, the sum over m in $B_U(f)$ is dominated by $m^*(f)$ giving the Arrhenius formula, $k_U(f) = k_0 \exp\big(-\frac{\Delta G_{m^*(f)}}{k_BT}\big)$ and $\Delta G_{m^*(f)} = G_{m^*(f)} - G_0$. In general, m^* depends on f leading to brittle (m^* small) or fragile (m^* large) behavior [29].

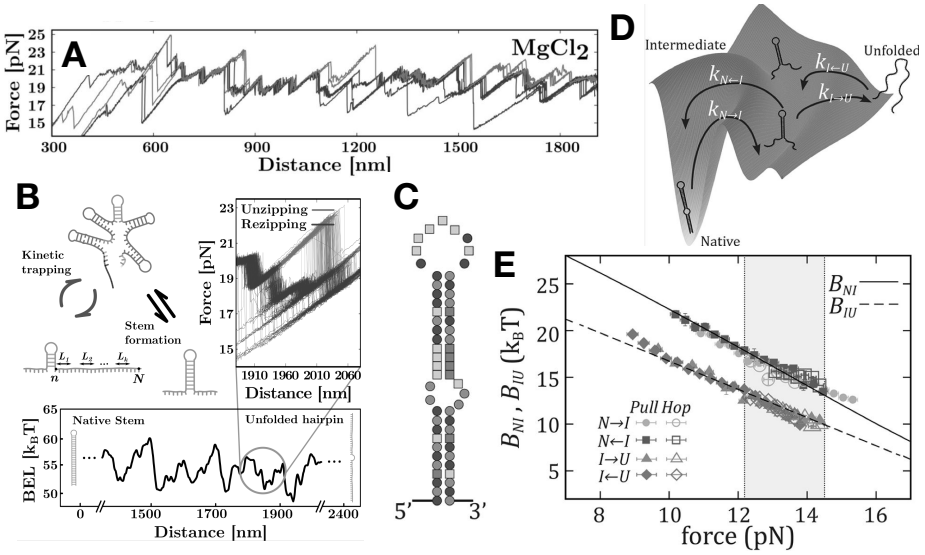

Fig. 27.2. Barrier energy landscapes. A) Unzipping (grey) and rezipping (black) FDCs of 2kbp RNA hairpin at 10mM $MgCl_2$ showing hysteresis. Data from Ref. [24]. B) The barrier energy landscape (BEL,bottom) is determined by stem-loops formed along the unpaired strands. C) A hairpin sequence with an internal loop produces a folding intermediate. D) Energy landscape showing different states and kinetic rates. E) Force-dependent kinetic barriers between different states (N, native; I, intermediate; U, unfolded) obtained from kinetic rates measured in nonequilibrium pulling (Pull) and equilibrium hopping (Hop) compared to the Kramers formula Eq.(27.2).Data in C,D,E from Ref. [26]

Equation (27.2) has been used to derive k_0 and the folding free energy of NA hairpins (Figure 27.2C) in free energy landscapes with one intermediate (Figure 27.2D). The barrier to unfold $B_U(f)$, and the equivalent one to fold $B_F(f)$ (obtained by transforming $m \to -m$ in Eq.(27.2)), fulfill detailed balance, $\Delta G_N(f) = B_U(f) - B_F(f)$. Experimental measurement of $k_U(f), k_F(f)$ permit us to calculate $B_U(f), B_F(f)$ (Eq.(27.2), lhs) and derive $\Delta G_N(f)$ by matching the profiles of $B_U(f)$ and $B_U(f) + \Delta G_N(f)$. The Continuous Effective Barrier Approach (CEBA) works well for deriving free energy differences of NA hairpins with multiple intermediates and pathways [26].

The mathematical expression for $B_U(f)$ in Eq.(27.2) reminds of a partition function or potential of mean force. For disordered landscapes, $B_U(f)$ is sensitive to small changes in the energies explaining the strong dependence of folding kinetics with NA sequence. Equation (27.2) cannot explain the irreversibility observed in Fig.27.2A, particularly upon upon comparing with the DNA case (Fig.27.1A). Off-pathway structures are then needed to estimate barrier energy landscapes, a difficult problem without reliable tertiary RNA prediction tools.

27.4. From NAs to protein folding

Randomized ssDNA folds into heterogeneous structures. To investigate ssDNA folding, we use the blocking oligo method [30, 31] in which a specifically designed 20-30b oligo hybridizes with the loop region preventing hairpin reannealing below 15 pN (Fig.27.3A).

A helix-coil model [32] of compact and free alternating regions describes the pulling curves at different salt conditions (Fig.27.3B). The model contains two parameters: the energy gain per base in a compact domain, ϵ, and the cooperativity parameter γ for the interfacial energy of a domain wall separating compact and free regions. The compact regions formed by the ssDNA are heterogeneous blobs containing 10-30 bases on average. More important, the cooperativity parameter is salt independent $\sim$0.7kcal/mol (Fig.27.3C), and larger than the energy per base in compact regions, $\epsilon \sim 0-0.2$ kcal/mol. Parameters γ, ϵ are equivalent to the magnetic field h and exchange coupling J in the 1D Ising model, showing that cooperativity drives non-specific secondary structure formation in ssDNA.

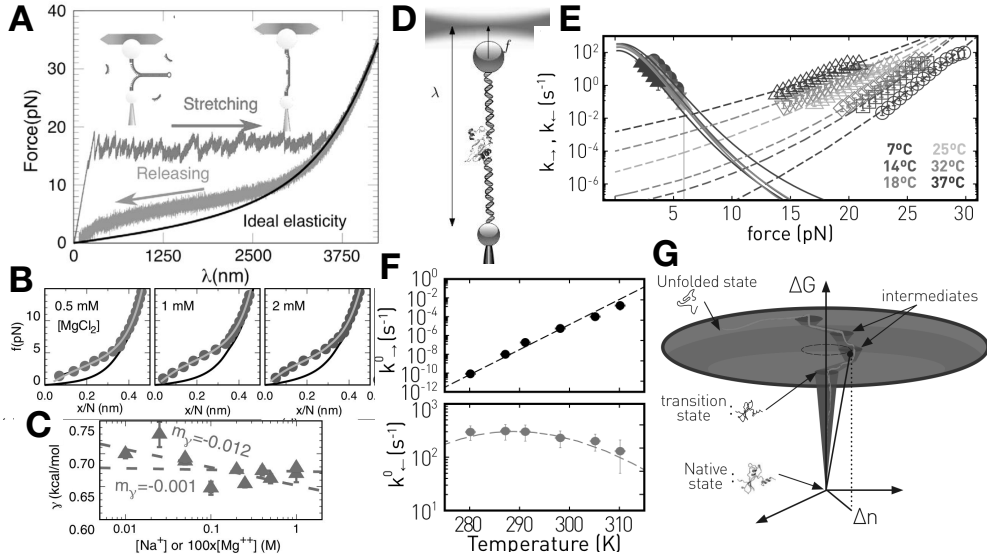

Fig. 27.3. ssDNA and protein folding. A) ssDNA unzipping and the blocking oligo method. Deviations of the releasing FDC from the ideal elastic response are due to non-specific secondary structure formation. B) Helix coil model fits (continuous light color lines) to the experimental force versus extension/base data in magnesium (dots). The back line is the ideal elastic response obtained by measurements in glyoxal. C) Cooperative parameter γ fitted to $\gamma = \gamma_0 + m_\gamma \log(c)$ with c the salt concentration in molar units (dashed lines). The value of $m_\gamma \ll \gamma_0 (= \gamma(c = 1))$ (both in kcal/mol) shows weak salt dependence. D) Pulling a protein using dsDNA handles. E) Calorimetric force spectroscopy measurements of unfolding (empty symbols) and folding (filled symbols) kinetic rates at various temperatures fitted to the Bell-Evans model (dashed lines). F) Extrapolated rates at zero force. G) Funnel free energy landscape representation where the z-axis stands for the free energy and the x-y plane the change in the number of degrees of freedom n upon folding. The latter is related to the measured heat capacity change, $\Delta C_p = k_B \Delta n/2$. A-C data from Ref. [32]. D-G data from Ref. [33]

Cooperativity is also key in protein folding. In the *foldon* hypothesis (FH), amino acids chains fold by forming compact units (foldons) sequentially and cooperatively [34, 35]. In the energy landscape hypothesis (ELH), there are multiple folding pathways connecting the unfolded (U) chain and the native (N) state in a funnel-like or golf-course energy landscape [36, 37]. The hole in that landscape represents the transition state (TS) that precedes folding to N. The nature of TS has been long debated. In the molten

globule hypothesis (MGH) the TS is a native-like expanded structure with the backbone formed, but with side chains loosely packed [38, 39]. Related to the ELH is the downhill hypothesis (DH) where folding is barrierless even in two-state proteins [40].

Protein folding kinetics can be measured by calorimetric force spectroscopy carrying out pulling experiments (Fig.27.3D) at different temperatures (5-40$^{\mathrm{o}}$C) using a temperature jump optical trap [41]. Figure 27.3E shows measurements of the force-dependent kinetic rates in the 110 amino acids protein barnase [33, 42]. Unfolding and folding kinetics rates were extrapolated to zero force (continuous lines) using the Bell-Evans model combined with the temperature-dependent elastic properties of the polypeptide chain. While the unfolding kinetic rate $k_{\rightarrow}$ changes by ten decades over the explored temperature range, the folding rate $k_{\leftarrow}$ is nearly temperature independent (Fig.27.3F). These results support the ELH, where the unfolded chain folds into to a molten globule first (the hole of the landscape), followed by the collapse of the molten globule into N (Fig.27.3G). It was found [33] that 80% of the free energy, enthalpy and entropy of folding of barnase occurs in the collapse between TS and N, whereas 90% of the total folding heat capacity change, $\Delta C_p \sim$1000cal/(mol K), occurs between U and TS. These results highlight a TS of high energy and low configurational entropy that is structurally similar to N. Barnase is an example of a protein where the FH,ELH,MGH and DH are compatible. We emphasize the close connection between protein folding and the first-order RSB transition in structural glasses [43]. The loss of the configurational entropy (also denoted as complexity) between U and TS defines a transition between a disordered paramagnetic phase (the unfolded chain) and a spin-glass phase (molten globule) where side chains are rightly positioned in space but loosely packed. The transition between the molten globule and N is a *solidification* transition driven by enthalpy and entropy collapse.

The folding kinetics of biomolecules and spin glasses share much in common. Endowed with single-molecule tools, scientists can now monitor folding events one molecule at a time and test the most elusive predictions of RSB. In 1969, Levinthal noticed a polypeptide chain could not fold into the native state by random search in configurational space [44]. The configurational space of biomolecules is large enough to abide by the tenets of spin glass theory [45]. Single-molecule research offers a terrific playground for a future test of its most notable predictions.

Acknowledgments

I am indebted to my mentor and friend, Giorgio Parisi, for his guidance and wisdom during my beautiful years in Rome (1989-1994) and after. Financial support from project PID2019-111148GB-I00 (Spanish Research Council) and Icrea Academia Prize 2018 (Catalan Government) is acknowledged.

References

[1] C. Calladine, H. Drew, B. Luisi, and A. Travers, Understanding dna: The molecule and how it works. 2004, *London and San Diego: Elsevier Academic Press.[Google Scholar]*.

[2] A. Pyle, Metal ions in the structure and function of rna, *JBIC Journal of Biological Inorganic Chemistry*. **7**(7), 679–690, (2002).

[3] P. Auffinger, N. Grover, and E. Westhof, Metal ion binding to rna, *Met Ions Life Sci.* **9** (1), 9781849732512–00001, (2011).
[4] J. Lipfert, S. Doniach, R. Das, and D. Herschlag, Understanding nucleic acid–ion interactions, *Annual review of biochemistry.* **83**, 813, (2014).
[5] K. A. Dill and J. L. MacCallum, The protein-folding problem, 50 years on, *science.* **338** (6110), 1042–1046, (2012).
[6] K. A. Dill, S. Bromberg, and D. Stigter, *Molecular driving forces: statistical thermodynamics in biology, chemistry, physics, and nanoscience.* (Garland Science, 2010).
[7] A. Cavagna, Supercooled liquids for pedestrians, *Physics Reports.* **476**(4-6), 51–124, (2009).
[8] P. G. Debenedetti, Supercooled and glassy water, *Journal of Physics: Condensed Matter.* **15**(45), R1669, (2003).
[9] M. Mezard and A. Montanari, *Information, physics, and computation.* (Oxford University Press, 2009).
[10] F. Ritort, Single-molecule experiments in biological physics: methods and applications, *Journal of Physics: Condensed Matter.* **18**(32), R531, (2006).
[11] C. J. Bustamante, Y. R. Chemla, S. Liu, and M. D. Wang, Optical tweezers in single-molecule biophysics, *Nature Reviews Methods Primers.* **1**(1), 1–29, (2021).
[12] K. C. Neuman, T. Lionnet, and J.-F. Allemand, Single-molecule micromanipulation techniques, *Annual Review of Materials Research.* **37**(1), 33–67, (2007).
[13] H. Miller, Z. Zhou, J. Shepherd, A. J. Wollman, and M. C. Leake, Single-molecule techniques in biophysics: a review of the progress in methods and applications, *Reports on Progress in Physics.* **81**(2), 024601, (2017).
[14] J. R. Moffitt, Y. R. Chemla, S. B. Smith, and C. Bustamante, Recent advances in optical tweezers, *Annu. Rev. Biochem.* **77**, 205–228, (2008).
[15] J. Gieseler, J. R. Gomez-Solano, A. Magazzù, I. P. Castillo, L. P. García, M. Gironella-Torrent, X. Viader-Godoy, F. Ritort, G. Pesce, A. V. Arzola, et al., Optical tweezers—from calibration to applications: a tutorial, *Advances in Optics and Photonics.* **13**(1), 74–241, (2021).
[16] B. Essevaz-Roulet, U. Bockelmann, and F. Heslot, Mechanical separation of the complementary strands of dna, *Proceedings of the National Academy of Sciences.* **94**(22), 11935–11940, (1997).
[17] M. Rief, H. Clausen-Schaumann, and H. E. Gaub, Sequence-dependent mechanics of single dna molecules, *Nature structural biology.* **6**(4), 346–349, (1999).
[18] J. M. Huguet, N. Forns, and F. Ritort, Statistical properties of metastable intermediates in dna unzipping, *Physical review letters.* **103**(24), 248106, (2009).
[19] J. SantaLucia Jr, A unified view of polymer, dumbbell, and oligonucleotide dna nearest-neighbor thermodynamics, *Proceedings of the National Academy of Sciences.* **95**(4), 1460–1465, (1998).
[20] J. M. Huguet, C. V. Bizarro, N. Forns, S. B. Smith, C. Bustamante, and F. Ritort, Single-molecule derivation of salt dependent base-pair free energies in dna, *Proceedings of the National Academy of Sciences.* **107**(35), 15431–15436, (2010).
[21] J. M. Huguet, M. Ribezzi-Crivellari, C. V. Bizarro, and F. Ritort, Derivation of nearest-neighbor dna parameters in magnesium from single molecule experiments, *Nucleic acids research.* **45**(22), 12921–12931, (2017).
[22] D. Thirumalai and S. Woodson, Kinetics of folding of proteins and rna, *Accounts of chemical research.* **29**(9), 433–439, (1996).
[23] N. B. Leontis, A. Lescoute, and E. Westhof, The building blocks and motifs of rna architecture, *Current opinion in structural biology.* **16**(3), 279–287, (2006).
[24] P. Rissone, C. V. Bizarro, and F. Ritort, Stem–loop formation drives rna folding in mechanical unzipping experiments, *Proceedings of the National Academy of Sciences.* **119** (3), e2025575119, (2022).

[25] P. Rissone and F. Ritort, Nucleic acid thermodynamics derived from mechanical unzipping experiments, *Life*. **12**(7), 1089, (2022).
[26] M. Rico-Pasto, A. Alemany, and F. Ritort, Force-dependent folding kinetics of single molecules with multiple intermediates and pathways, *The Journal of Physical Chemistry Letters*. **13**(4), 1025–1032, (2022).
[27] R. Zwanzig, *Nonequilibrium statistical mechanics*. (Oxford university press, 2001).
[28] M. Manosas, D. Collin, and F. Ritort, Force-dependent fragility in rna hairpins, *Physical Review Letters*. **96**(21), 218301, (2006).
[29] A. Alemany and F. Ritort, Force-dependent folding and unfolding kinetics in dna hairpins reveals transition-state displacements along a single pathway, *The journal of physical chemistry letters*. **8**(5), 895–900, (2017).
[30] M. Manosas, X. G. Xi, D. Bensimon, and V. Croquette, Active and passive mechanisms of helicases, *Nucleic acids research*. **38**(16), 5518–5526, (2010).
[31] A. Bosco, J. Camunas-Soler, and F. Ritort, Elastic properties and secondary structure formation of single-stranded dna at monovalent and divalent salt conditions, *Nucleic acids research*. **42**(3), 2064–2074, (2014).
[32] X. Viader-Godoy, C. Pulido, B. Ibarra, M. Manosas, and F. Ritort, Cooperativity-dependent folding of single-stranded dna, *Physical Review X*. **11**(3), 031037, (2021).
[33] M. Rico-Pasto, A. Zaltron, S. J. Davis, S. Frutos, and F. Ritort, Molten globule–like transition state of protein barnase measured with calorimetric force spectroscopy, *Proceedings of the National Academy of Sciences*. **119**(11), e2112382119, (2022).
[34] R. L. Baldwin, The nature of protein folding pathways: the classical versus the new view, *Journal of biomolecular NMR*. **5**(2), 103–109, (1995).
[35] H. Maity, M. Maity, M. M. Krishna, L. Mayne, and S. W. Englander, Protein folding: the stepwise assembly of foldon units, *Proceedings of the National Academy of Sciences*. **102** (13), 4741–4746, (2005).
[36] H. Frauenfelder, S. G. Sligar, and P. G. Wolynes, The energy landscapes and motions of proteins, *Science*. **254**(5038), 1598–1603, (1991).
[37] J. D. Bryngelson, J. N. Onuchic, N. D. Socci, and P. G. Wolynes, Funnels, pathways, and the energy landscape of protein folding: a synthesis, *Proteins: Structure, Function, and Bioinformatics*. **21**(3), 167–195, (1995).
[38] O. Ptitsyn, Molten globule and protein folding, *Advances in protein chemistry*. **47**, 83–229, (1995).
[39] R. L. Baldwin and G. D. Rose, Molten globules, entropy-driven conformational change and protein folding, *Current opinion in structural biology*. **23**(1), 4–10, (2013).
[40] W. A. Eaton, Searching for "downhill scenarios" in protein folding, *Proceedings of the National Academy of Sciences*. **96**(11), 5897–5899, (1999).
[41] S. De Lorenzo, M. Ribezzi-Crivellari, J. R. Arias-Gonzalez, S. B. Smith, and F. Ritort, A temperature-jump optical trap for single-molecule manipulation, *Biophysical journal*. **108**(12), 2854–2864, (2015).
[42] A. Alemany, B. Rey-Serra, S. Frutos, C. Cecconi, and F. Ritort, Mechanical folding and unfolding of protein barnase at the single-molecule level, *Biophysical journal*. **110**(1), 63–74, (2016).
[43] T. Kirkpatrick and D. Thirumalai, Colloquium: Random first order transition theory concepts in biology and physics, *Reviews of Modern Physics*. **87**(1), 183, (2015).
[44] C. Levinthal, Are there pathways for protein folding?, *Journal de chimie physique*. **65**, 44–45, (1968).
[45] M. Mézard, G. Parisi, and M. A. Virasoro, *Spin glass theory and beyond: An Introduction to the Replica Method and Its Applications*. vol. 9, (World Scientific Publishing Company, 1987).